C. R. Chimie 17 (2014) 342–351

Contents lists available at ScienceDirect

Comptes Rendus Chimie

www.sciencedirect.com

Full paper/Mémoire

A systematic methodology to design silica templates: Silica microemulsion formulation and nanodroplet type and size estimation

Maria Mihaly [a], Ioana Lacatusu [b], Nicoleta-Liliana Olteanu [c], Aurelia Meghea [c,*]

[a] University Politehnica of Bucharest, Faculty of Applied Chemistry and Materials Science, Inorganic Chemistry, Physical Chemistry and Electrochemistry Department, Polizu 1, 011061, Bucharest, Romania
[b] University Politehnica of Bucharest, Faculty of Applied Chemistry and Materials Science, C.D. Nenitescu Organic Chemistry Department, Polizu 1, 011061, Bucharest, Romania
[c] University Politehnica of Bucharest, Research Centre for Environmental Protection and Eco-friendly Technologies, Polizu 1, 011061, Bucharest, Romania

ARTICLE INFO

Article history:
Received 6 March 2013
Accepted after revision 30 September 2013
Available online 20 February 2014

Keywords:
Silica-microemulsion template
Phase diagram
Phase inversion point
Phase inversion temperature
Inorganic and/or hybrid silica materials

ABSTRACT

A systematic study of the design and characterization of silica-microemulsion templates is presented. The ternary phase diagrams in micro-heterogeneous systems, by using a non-ionic surfactant (Brij 30) and different silica precursors (MTEOS, TEOS, PTEOS), have been drawn. Based on Khalweit diagrams, the phase inversion temperature was estimated as close to 315 K, for both alchil (TEOS) and aril (PTEOS) types of alcoxides. By correlating the information obtained from phase diagrams at room temperature with that of size effects revealed by VIS absorption molecular probes (bromthymol blue dye), the phase inversion point, i.e. the transition point from water-in-oil to oil-in-water microemulsion, was also clearly established as corresponding to $R \sim 1$. Besides technically attractive features such as a wide variety of inorganic and hybrid nanomaterials, high specific surface and highly efficient applicative properties of the final materials, the approach of silica-microemulsion-based templates can be seen as a route towards the *Green Chemistry* concept.

1. Introduction

The study and research of silica have emerged with a special importance in science and technology, both in processing and utilization, due to its extensive application in the field of catalysis [1–10], separation [4,11–13], electronics [4,14,15], and biotechnology [4,13,16].

In the area of the exploration of applications, the use of silica benefits a great deal from its porous structure, high specific surface area, high thermal stability, optical transparency, and chemical inertness. However, pure silica mesoporous materials exhibit low catalytic activity, no selective adsorption properties, and isolating characteristics. Therefore, one of the emerging trends is to improve their properties by immobilization of functional components onto the silica support. These silica-based nanomaterials combine the excellent properties of mesoporous silica with the special properties of functional components (i.e. metallic or/and metallic oxides nanoparticles, chromophores, biomolecules), resulting in multifunctional nanomaterials with specific applications.

As the uniform distribution of active components on silica surfaces is a challenge, several procedures have been reported. Among them, impregnation [17–19], grafting by L–S reaction or G–S reaction [20–24], isomorphous substitution [25–28], molecular design dispersion approach [29,30], template ion-exchange method [31,32] and microemulsion assisted sol–gel technique [1,33–39]. The last technique is related to the incorporation of inorganic and/or organic functional entities within the microemulsion

* Corresponding author.
E-mail address: a.meghea@gmail.com (A. Meghea).

1631-0748/$ – see front matter
http://dx.doi.org/10.1016/j.crci.2013.09.018

colloidal aggregates, acting as templates for both nanoparticles synthesis and silica nanostructured network.

This technique has some important strong points [32,33,38,40], as: (i) the suitability for hybrid silica nanomaterials synthesis using microemulsion to enhance the solubility of hydrophobic active compounds and to provide a readily controlled, stable medium for the solubilized components, together, perhaps, with protection against degradation; (ii) the possibility to control the composition, size and shape of nanoparticles and to avoid their aggregation, resulting into a high degree of homogeneity and monodispersity of the final material; (iii) the minimization and/or managing by-products by replacing multistep processes by direct schemes, reducing effluents (solvents) and processing the final materials as films, all of them being in agreement with the *Green Chemistry* concept.

As the use of microemulsions as templates should lead to nanomaterials with high surface area and structure similar to that of the template, the microemulsion formulation and its control became a very tough issue. Formulation is mainly related to the working variables (T and p) and composition variables (the relative amount of the different substances present in the system) that influence the microemulsion properties sometimes to quite a large extent. An accurate handling formulation is extremely useful, not only to prepare microemulsion, but it is also directly linked with their properties such as type, stability, viscosity, and drop size.

Based on these essential features of the microemulsion template and silica material itself, and having in view the limited literature [41] that illustrates the use of phase diagrams for identifying appropriate single-phase microemulsions, a comprehensive and applied approach involving non-ionic surfactants self-assembling at the water/alcoxide interface is presented in this paper. Analysing thoroughly ternary phase diagrams and highlighting their unique features are extremely useful to know how to insert silica into homogeneous nanostructures, able to incorporate functional components, thus resulting in inorganic or hybrid nanomaterials, as powders or thin films, for the target applications.

In this context, the present work deals with the phase behaviour in ternary systems containing alcoxides, as oil phase, water, and a non-ionic surfactant, polyoxyethylene-4-lauryl ether (Brij 30), which makes them compatible. The primary goal of this study is to find the appropriate conditions under which different types of microemulsions are formed and their phase transition, which might result in a variety of silica templates. Firstly, the phase diagrams of the corresponding ternary water/Brij 30/alcoxide systems have been drawn. Since the effect of pressure on the phase behaviour is generally insignificant [42], only the effect of temperature has been studied. The phase inversion temperature (PIT) was evaluated using the Khalweit diagram. As the local environment of entrapment structures might affect the stability and functionality of the final materials, the polarity of nanoenvironments has been only investigated by using a UV–Vis absorption molecular probe and the phase inversion point (PIP) has been evaluated. Based on the size effect revealed in the nanostructured silica-microemulsion templates, the sizes of the nanodroplets were estimated.

2. Experimental

2.1. Materials

Polyoxyethylene-4-lauryl ether (Brij 30), hydrochloric acid (HCl), and sodium hydroxide (NaOH) were purchased from Sigma; bromthymol blue dye (BTB), trimethoxymetilsilane (MTEOS), tetraethoxysilane (TEOS), and trimethoxy(phenyl)silane (PTEOS) were purchased from Merck; ultra-pure water (Millipore Corporation) was used.

2.2. Construction of phase diagrams

Several ratios between the mass of the immiscible components ($R = m_w/m_o$) have been titrated with different proportions of surfactant, corresponding to the phase transitions in water/surfactant/oil system. Then, for establishing the PIT, the Khalweit diagrams have been built in the 17–60 °C temperature range, at a constant mass ratio, R, alcoxide:water (3:2), according to the overall reaction stoichiometry of the sol–gel process (1 mol TEOS: 2 mol H_2O). The samples were taken in sealed test tubes and shaken vigorously, using a magnetic stirrer to ensure proper mixing, and then kept in a thermostatic device at the desired temperature. The phase transitions in the studied systems have been visually inspected by using a VIS absorption molecular probe, BTB dye.

2.3. Investigations of local environment and size effect in silica-microemulsion templates

Different amounts of water, denoted by $W = [H_2O]/[\text{Brij 30}]$ (w/w), were added to 25% (w/w) surfactant alcoxidic solutions. After a few minutes of mechanical stirring, the resulted microemulsions have been subjected to UV–Vis analysis. Vis electronic spectra of samples held in 1-cm path length quartz have been recorded at a wavelength domain ranging from 360 to 800 nm using a Jasco double-beam V570 spectrophotometer. The spectral investigation of the new silica templates is based on the absorption maxima shifts of Vis absorption molecular probe. The molecular probe, bromthymol blue dye (BTB), was introduced in samples using the following procedure: an appropriate amount of stock ethanol solution was evaporated directly into the cells, before the samples were added. The lowest value of W ($W = 0$) is attributed to the system without water, and the highest value was registered before and after the separation of phases at 25 °C.

3. Results

3.1. Phase diagrams in the ternary system water/Brij 30/alcoxide

Understanding the importance of the formulation in determining the phase behaviour is often achieved by

using a simplified description of what happens at the water/oil interface. The phase behaviour at equilibrium is interpreted through the so-called ratio R between the amounts of the immiscible components and the surfactant concentration, as it is illustrated in Scheme 1 [41]. Even though R is a quantitative parameter, it does not count as a condition depending on all formulation variables, but could be used to interpret the phase transitions of water/surfactant/alcoxide systems and somehow to assess the change of microemulsion properties.

A microemulsion is commonly known as a nanodispersion of water into oil or oil into water, stabilized by an interfacial self-assembled membrane formed by surfactant molecules. There are four multiphase domains according to Winsor classification. In the presence of an excess of oil, the microemulsion oil-in-water (O/W) coexists with an upper oil continuous phase and Winsor-I type is formed (WI, two-phases (O/W, O)), while with an excess of water, the water-in-oil phase coexists with an aqueous continuous one (WII, two-phases (W/O, W)). In Winsor III type (WIII), three phases are present, where the microemulsion (μE) is in equilibrium with both excess aqueous and organic phases (W, μE, O), and in Winsor IV type (W/O, O/W or both), only a microemulsion phase is formed [43].

For lower concentrations of surfactant, below micelles critical concentration (MCC), the number of molecules at the water/oil interface is small and thus its capacity to form and stabilize micelles (droplets) is reduced. Above MCC, and at still lower surfactant concentrations, the droplets will be formed and put together to give a continuous phase in a small volume equilibrated by a poor-surfactant phase. If $V_W/V_O > 1$, then $V_W/V_{SF} < V_O/V_{SF}$ and the predominant interactions will be hydrophilic, having a convex interphase with respect to water (reverse micelles) ($R > 1$). As a result, a W II system will be formed (W/O microemulsion phase in equilibrium with a lower poor-surfactant water phase). In the opposite side of the diagram, where $V_W/V_O < 1$, then $V_W/V_{SF} > V_O/V_{SF}$, and the interactions will be mainly lipophilic and a Winsor-I system will appear (O/W microemulsion phase in equilibrium with an upper poor-surfactant oil phase) as a consequence of a convex interface formation with respect to oil (direct micelles) ($R < 1$). When $R = 1$, the affinities of the surfactant for the two media are comparable with each other, $V_W/V_{SF} = V_O/V_{SF}$, and W-III microemulsion is formed. The surfactant solubilizes equal amounts of water and oil ($R = 1$) and is in equilibrium with the two aqueous and organic phases in excess.

When the surfactant concentration is increasing, both hydrophilic and lipophilic interactions are affected, and the inversion of phases occurs. For a ratio $V_W/V_O < 1$, water will hydrate the oxyethylenic groups, as it will no longer solubilise the surfactant. In this case, hydrophilic interactions will predominate, R will become higher than unity and the resulting one-phase microemulsion is similar to the system of reverse micelles. For $V_W/V_O > 1$, the contact surface with water is increasing, while that with oil is decreasing. As a consequence, the lipophilic interactions become more important and determine the inversion of the interface geometry: it will no longer be convex towards water ($R > 1$), but convex towards oil ($R < 1$); as a result, W-IV microemulsion will be formed in a similar fashion to the system consisting of direct micelles.

When $R = 1$, isotropic systems are formed that contain aggregates similar to both direct and indirect micelles, relatively equal proportions of water and oil being solubilised. At a surfactant concentration still higher, but close to $R = 1$, its solubilising capacity is significantly higher, the interface towards oil is planar, and isotropic rigid structures, gels or liquid crystals, are formed.

By comparing the main behaviour of all studied systems (Fig. 1), one can easily observe that the change in the R ratio, from $R < 1$ to $R > 1$, could be associated with the phase transition from microemulsion type I (W I) to type II

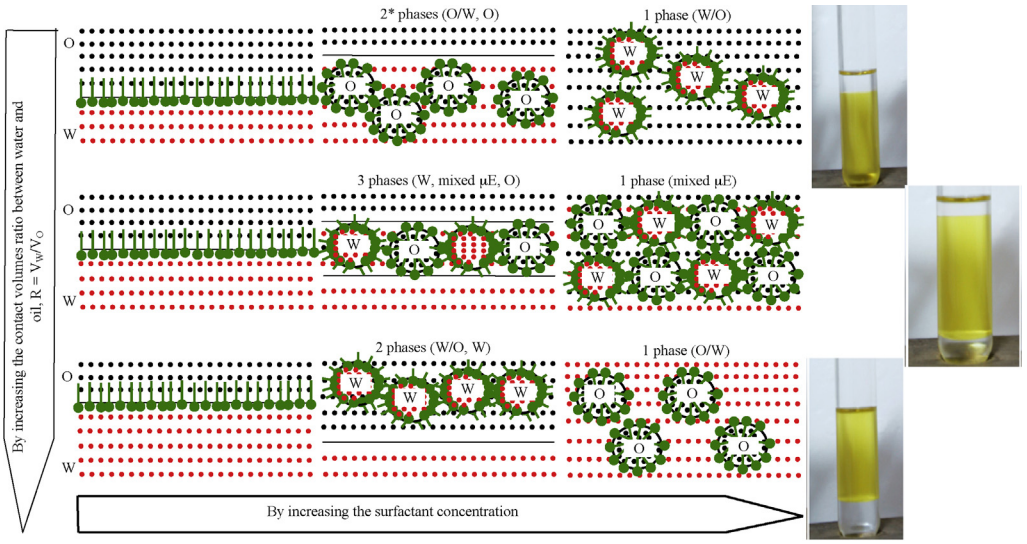

Scheme 1. (Color online.) Phase transitions in ternary system water (W)/surfactant (SF)/oil (O) associated with microemulsions: 1 phase–micellar solution (reverse or direct), W-IV microemulsion, gel or liquid crystals; 2 phases*–W-I type (O/W, O); 2 phases–W-II type (W/O, W); 3 phases–W-III type (W, μE, O). Reproduced with permission [41].

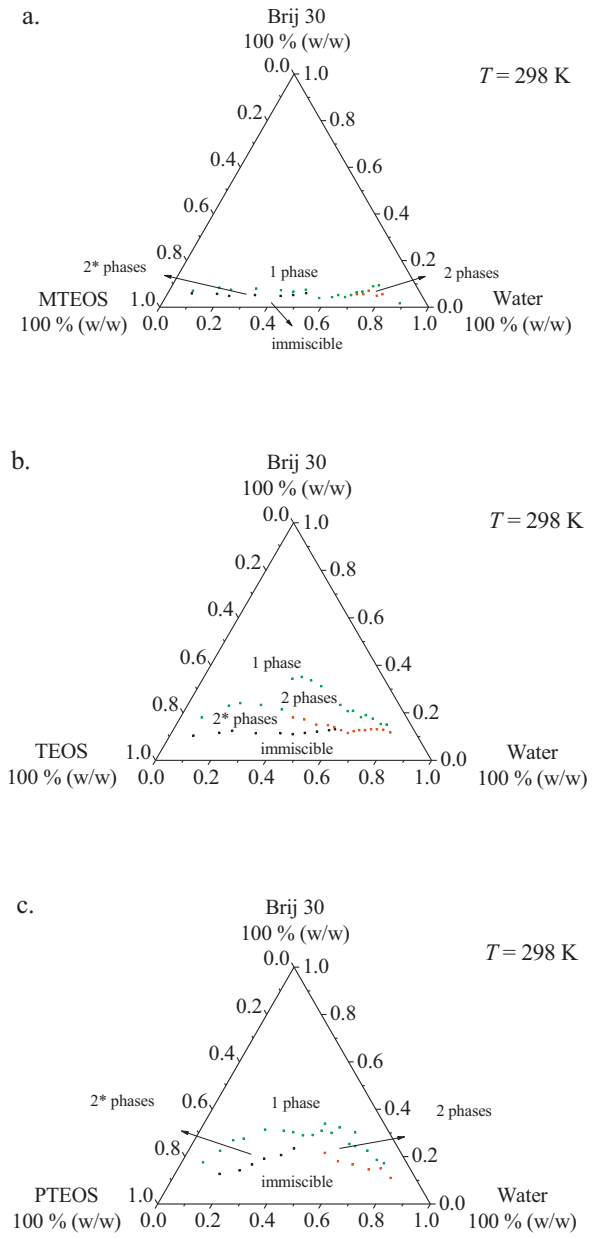

Fig. 1. Phase diagrams in ternary system at 298 K: 1 phase–micellar solution (reverse or direct), microemulsion W IV type, gel or liquid crystals; 2* phases–W-I type (O/W, O); 2 phases–W-II type (W/O, W); 3 phases–W-III type (W, μE, O).

(W II), while $R = 1$ corresponds to equal amounts of alcoxide and water.

For the studied systems, $R = 1$ seems to signify not only a mass ratio, but a measure of the neutral affinity of the Brij 30 surfactant for both alcoxide and water phases. Moreover, the water/surfactant/alcoxide systems involving alchil alcoxides (MTEOS, TEOS) are able to reach the optimum formulation, namely after the co-solubilisation of approximately equal amounts of alcoxide and water, with less than 10% surfactant, in the former case (MTEOS) and less than 20%, in the latter one (TEOS). Therefore, the use of the bicontinuous structure corresponding to the optimum formulation, when both types of droplets can be utilised for the synthesis and/or incorporation of both hydrophilic and hydrophobic components, is a very important aspect in the successful application of microemulsions as templates for silica-based nanomaterials. This is expected to lead to nanoporous silica-based materials with continuous internal surface and high specific surface area materials.

When compared to a similar ternary system containing another surfactant, Triton X-114 [41], the water/Brij 30/alcoxide systems based on alchil alcoxides require lesser amounts of surfactant in order to form the one-phase microemulsion type (W IV), while in the same time, it allows one to promote the phase transition from W-I to W-II types. By using MTEOS as oil phase, the area of W-I and W-II microemulsion types is much smaller and begins at lower surfactant concentrations (~5%, for the water/Brij 30/MTEOS system respectively ~7%, water/TX-114/MTEOS system). These results reveal the extension of the single-phase area (over 10% for the water/Brij 30/MTEOS system, and from 17 to 30%, for water/TX-114/MTEOS system, respectively). A very narrow range obtained for the water/Brij 30/MTEOS system, as compared to water/TX-114/MTEOS, could be attributed to the aliphatic character of Brij 30/MTEOS compounds. The aromatic character of TX-114 weakens its affinity towards MTEOS, thus leading to a decrease of its solubility in alcoxide solution. This behaviour could be explained by correlating the alchil/aril character, imprinted by the surfactant type, with strengthening of the alcoxide hydrophobicity in the series MTEOS < TEOS < PTEOS.

Regarding the phase diagrams for water/Brij 30/PTEOS systems (Fig. 1c), a higher surfactant concentration is needed to stabilise both WI and WII microemulsion types, thus inducing a decrease of their formation areas. Compared to the phase behaviour of similar ternary system with TX–114, this system forms a one-phase microemulsion at higher concentrations of the Brij 30 surfactant, but it has the advantage to allow the formation of two-phase microemulsion ranges.

Moreover, the use of water/Brij 30/alcoxide microemulsion as a template has the advantage of leading to both inorganic (in case of water-in-oil microemulsion) and hybrid (in case of using oil-in-water microemulsion) silica-based nanomaterials, either as silica-coated nanoparticles or silica films doped with functional components.

In our previous work [33], DNA-silica based nanomaterials with ordered units' array pattern have been obtained by immobilization of DNA in a silica matrix using silica-microemulsion based templates. This incorporation of DNA has led to the conservation of the structural properties of native DNA, while improving its thermal resistance. The DNA has a globular structure in the silica matrix, determined and stabilized by water-in-oil microemulsion droplets, which enhanced the chromophore (also incorporated into the matrix) alignment, even at low concentrations of DNA bio-molecules of about 0.15%. Thus both linear and nonlinear optical properties of the systems [44] were significantly increased. More specifically, the addition of DNA has been found to result

in higher transmittance and fluorescence efficiency, as well as significantly higher third-order nonlinearity.

The feasibility of using these silica-microemulsion-based templates was once more tested by authors [34] when NiO-silica-based nanomaterials have been synthesized (silica-coated NiO nanoparticles and NiO embedded in silica film) using water-in-oil microemulsion. K. Kouachi et al. [1] and T. Aubert et al. [39] also prepared silica-supported nanomaterials using a similar procedure. The nanomaterials thus obtained present highly homogenous dispersed nanoparticles on the silica support in contrast with impregnated silica materials.

Therefore, the oil-in-water microemulsion represents a unique tool to obtain highly homogeneous hybrid silica materials [35]. The authors used this way to prepare fullerene C_{60} clusters-silica-based hybrid nanomaterials (silica-coated C_{60} nanoclusters or C_{60} doped silica films) by inversing the oil-in-water microemulsion, which represents the single method for obtaining monomodal C_{60} nanoclusters, with water-in-oil type, as proper environment for silica network formation. These materials also exhibit improved photostability and high specific surface area, which leads to increased adsorption efficiency. In addition to these properties, their band-gap energies are below 3 eV, meaning that they are able to absorb visible or near-UV light, which recommends such materials as potential photocatalysts.

Finally, the use of microemulsion at optimal formulation as a template should lead to a silica-based material suitable for a wide range of application that require rapid and responsive sampling, selective separation, high throughput catalytic processing, or enhanced chemical activity.

3.2. Temperature effect on phase equilibrium and on dispersion type in non-ionic ternary systems

The phase behaviour of the ternary system involving a non-ionic surfactant depending on the temperature results from the interplay between the lower miscibility of the oil-surfactant mixture and the upper miscibility of the water-surfactant mixture. At low temperature the non-ionic surfactant is mainly soluble in water, while at high temperatures it is mainly soluble in oil. Thus, an increase in temperature turns a non-ionic surfactant from hydrophilic into hydrophobic.

As a work-up approach, the concept is particularly useful for a microemulsion based on non-ionic surfactants, because the transitions obtained by temperature variation are reversible, thus extending the variety of templates.

A simple and extremely useful procedure to obtain an overview of the phase transition promoted by the temperature change is to draw the phase diagram at a constant oil/water ratio, *R*, as a function of temperature and surfactant concentration, the so-called Khalweit diagram. Such schematic diagram allows one to determine more easily the PIT, as the temperature where the surfactant induces the phase inversion from oil-in-water to water-in-oil microemulsion types.

Fig. 2 shows the influence of temperature on the phase transition for all studied water/surfactant/alcoxide systems, at a constant alcoxide:water (3:2) mass ratio. By microscopically inspection of these mixtures, at low temperature, one can find an amphiphilic film that forms an alcoxide-in-water microemulsion which coexists with an alcoxide excess phase (2 phases*, WI type). At high temperature, the inverted microemulsion is formed, when a water excess phase coexists with a water-in-alcoxide microemulsion (2 phases, WII type). At intermediate temperature, the surfactant is almost equally soluble in both solvents and a locally planar amphiphilic film is formed. Here, a surfactant-rich bicontinously structured phase (both water and alcoxide droplets) and excess alcoxide and water phases coexist (three phases, WIII type).

The PIT of water/surfactant/alcoxide systems, at constant mass ratio alcoxide:water (3:2), are presented in Table 1. One can notice that the PIT corresponds to an increasing surfactant concentration from ≃13% to 23% (TEOS < PTEOS) in agreement with the hydrophobicity increase and similar to that at room temperature.

Based on this behaviour, one can assume that all the systems, at a constant mass ratio alcoxide:water (3:2), could reach high efficiency at low surfactant concentration, in

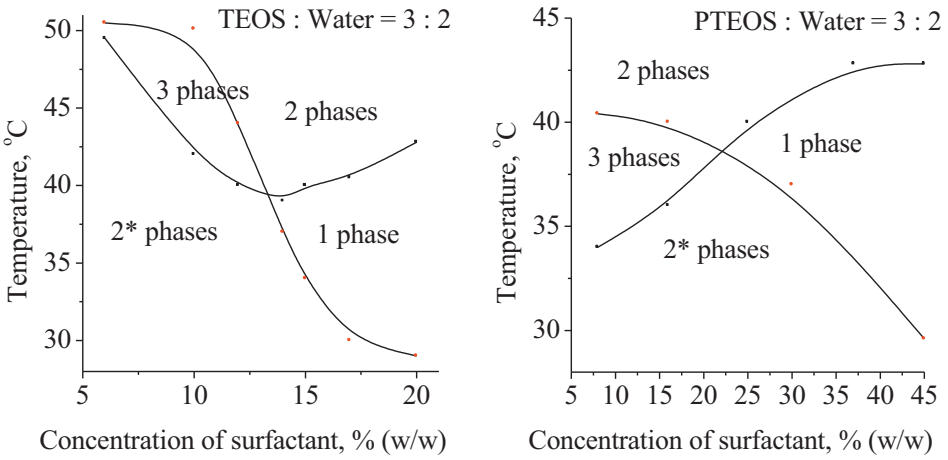

Fig. 2. Khalweit diagrams for ternary systems, at constant mass ratio alcoxide:water = 3:2.

Table 1
Phase inversion parameters for ternary systems at constant mass ratio alcoxide:water (3:2).

System	PIT K	Surfactant concentration %(w/w)
Water/Brij30/MTEOS	298	9
Water/Brij30/TEOS	312	13
Water/Brij30/PTEOS	311	23

terms of finding the microemulsion in which a minimum amount of surfactant is necessary for the alcoxides solubilisation in water or vice versa.

The increase in temperature leads to the formation of all types of microemulsion, including type III (three phases, WIII type).

Having in view all these aspects, and particularly the applicative impact of these silica-microemulsion-based templates, the phase diagrams for two alcoxides, TEOS and PTEOS, have been drawn at temperatures higher than PIT, 318 K and 315 K, respectively (Fig. 2).

Compared to the behavior at room temperature, one can notice that, in the TEOS case (Fig. 3a), with increasing temperature, the surfactant-rich water phase splits into two phases and the three-phase body appears, while in the PTEOS case this leads to the formation of an extended miscibility gap, indicating WII microemulsion type (Fig. 3b).

One can conclude that having discussed the general behaviour of microemulsion by studying simple ternary non-ionic systems of type water/surfactant/alcoxides, numerous formulations are available for multifunctional silica-based nanomaterials.

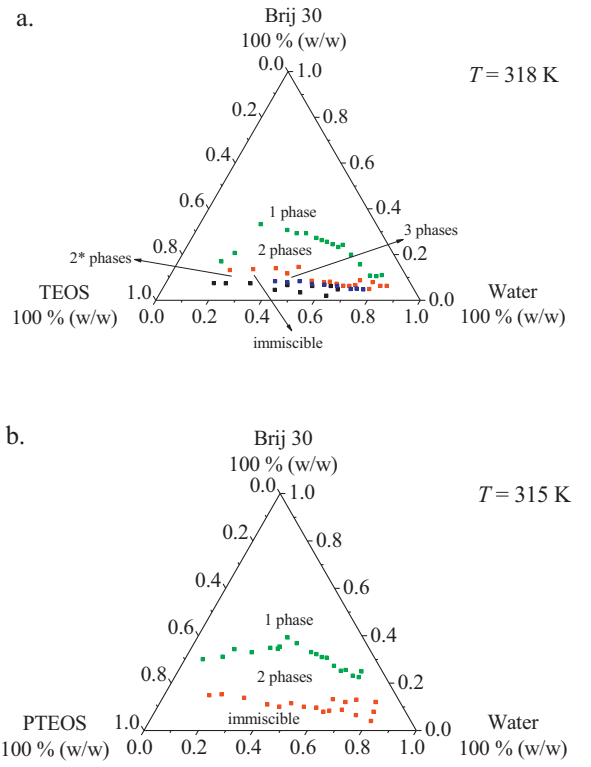

Fig. 3. (Color online.) Phase diagrams in a ternary system at a temperature close to PIT: 1 phase–micellar solution (reverse or direct), microemulsion W-IV type, gel or liquid crystals; 2 phases*–W-I type (O/W, O); 2 phases–W-II type (W/O, W); 3 phases–W-III type (W, μE, O).

3.3. Investigations of local microenvironment in micelles and microemulsions by using VIS absorption molecular probes

Most of the applications of microemulsions depend on the fact that these colloidal systems consist in a nanoscale heterogeneous topologically ordered interfacial film formed by the surfactant molecules at the water/oil interface. The nature and properties of these nanoscopic interfacial films are essential for the incorporation of different inorganic, organic, and biologic functional components.

A spectral investigation of micelles systems and the corresponding microemulsions has been performed by the VIS molecular probe technique using bromthymol blue (BTB) dye as the molecular probe, in order to study the structural and size effect in micelles and microemulsions [45,46]. The electronic transition energy of the probe molecule, as reflected by the wavelength of their absorption maxima λ_{max}, provides valuable information about the "polarity" of their microenvironment and, consequently, on their location.

In this respect, the spectral characteristics and tensioactive properties of BTB probe into well-established environments justify its choice as VIS molecular probe for structural investigations in water/surfactant/alcoxide ternary systems. Its specificity for such kind of investigations has been proven for the water/Brij 30/TEOS ternary system. The spectral parameters of BTB solutions, specific for each studied system—aqueous, organic (alcoxide–TEOS) and oxyethylenic surfactant (Brij 30)—are collected in Table 2.

3.3.1. Investigation of the local microenvironment in micelles

In order to localize the probe in micelles and microemulsions, several compositions of water/surfactant mixtures have been prepared, at surfactant concentrations below and above micelles critical concentration (MCC), with and without the alcoxide. The spectra obtained in these systems, at surfactant concentrations below MCC, exhibits the same absorption maxima as in pure aqueous solutions. By raising the surfactant concentration over MCC, when the number of micelle aggregates with nonpolar core is growing, the absorption maxima undergo a hipsochromic shift, suggesting a decrease in the polarity of the media. One can notice that the absorption maxima depend on the surfactant concentration (Supporting Information, Figure A).

The absorption spectra of BTB in organic solvents, at various concentrations of Brij 30, without water ($W = 0$), are characterized by the absorption band at $\lambda_{max} = 407.4$ nm. Compared to that in the pure surfactant, the absorption maxima in organic solution undergo a bathochromic shift, thus indicating a higher polarity of the media determined by the presence of some water molecules associated with

Table 2
Spectral parameters of BTB in different media [45].

Environment	Water	Brij 30	TEG	TEOS
λ, nm	430	407	416	400

the OE chains of the surfactant (Supporting Information, Figure B).

It is obvious that, below the MCC, BTB molecules are dissolved in the bulk water; however, above the MCC, the polar outer shell of the micelles composed of the hydrated OE chains is the suitable location for the probe. Extrapolating the conclusion for the aqueous surfactant solution to the analogous environment existing in the inverted structure of a W/O microemulsion droplet, one can affirm that BTB is located in the polar core of the aggregates.

3.3.2. Investigation of local microenvironment in microemulsions

Several microemulsions have been prepared by successive addition of water in an alcoxide solution of surfactant at a constant concentration. The electronic spectra recorded for these samples are presented in Figs. 4 and 5. The BTB probe in the water/Brij 30/TEOS system seems to be always placed within the surfactant OE groups region or distributed between this and the micelles core. For these reasons, the absorption spectra of BTB in TEG will be used as a reference.

3.3.2.1. Higher surfactant concentration (> 25%). For $R < 1$ and $W < 1$, due to the polarity inside the micelles, it can be assumed that the probe will be placed in the core, more exactly in the OE groups inner, and the BTB will not be solubilised in the existent water drops. This is proved by the bathochromic shifts (Fig. 4) of the maximum of the absorption spectra. In this area, reverse micelles and one-phase microemulsion of water-in-oil type are formed. For $R > 1$ and $W > 2$, oil-in-water microemulsions are formed by phase inversion. In this case, water becomes a continuous medium and the nonpolar core of the formed micellar aggregates contains organic solvent drops. A hipsochromic shift of the maximum absorption spectra for BTB/Brij 30 system ($\lambda_{max} = 399$ nm) is revealed in Fig. 4. This fact proved that the probe is distributed between the Brij 30 inner and the organic solvent drops without the solubilisation of BTB in the organic core of aggregates due to the fact that, with increasing W, the hydrophobic character of the aggregates core became predominant.

3.3.2.2. Lower surfactant concentration (10–25%). In this concentrations range of Brij 30, phase separation appears, and W-I and W-II type microemulsions are formed.

Fig. 5 reveals the evolution of the Brij 30/TEOS system when water is added. It started from W/O microemulsion, continued through the microemulsion characteristics of the W-II system, and finished with one-phase microemulsions of type O/W. The W/O microemulsion formation is proven by slight bathochromic shifts of the absorption maxima from $\lambda_{max} = 399$ nm ($R = 0$, $W = 0$) to $\lambda_{max} = 412.3$ nm, indicating the increase of the polarity due to the hydration of OE groups, and water drops formed.

Increasing W and R, the drops are swelling until the phase separation. In this way, W-II domain is obtained. The water is initially eliminated out of the microemulsion, thus becoming the dispersant agent. By getting together bigger and bigger water drops, the phase inversion occurs, and the O/W microemulsion is obtained.

Therefore, by using VIS absorption molecular probes, the nature of the droplet film, and, consequently, the type of microemulsion formed in water/Brij 30/TEOS system could be established. As the BTB probe presents specific absorption maxima in every studied media (Table 2), its location was appreciated to be always within the surfactant OE groups region or distributed between this and the micelles core. Therefore, based on these features of BTB, the phase inversion point has been estimated (Table 3).

The obtained results sustain the PIP estimation at a mass ratio alcoxide:water = (1:1), already estimated from the phase diagrams at room temperature.

3.3.3. Evaluation of size effect from spectral data

The size effects in microemulsions have been also appreciated using BTB as the Vis absorption molecular probe. Usually the formation of nanoparticles from microemulsions follows the template shape and size. The particle size is strongly related, in microemulsion, to i) the number of nanodroplets, ii) the concentration of precursor and iii) the interparticle interactions.

The nanostructures are referring to materials with a characteristic length scale in the lower nanometer range

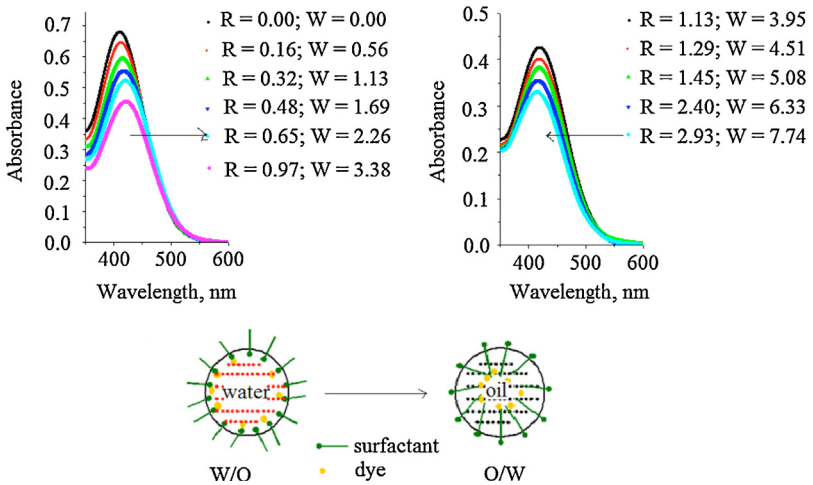

Fig. 4. (Color online.) Absorption spectra of water/Brij 30/TEOS system (single phase) vs. water content (W), at different water/oil ratios (R).

Table 3
PIPs for water/Brij 30/TEOS systems.

Surfactant concentration	Microemulsion type		
	W IV (water-in-oil) 1 phase	W II (water-in-oil, water excess) 2 phases	W IV (oil-in-water) 1 phase
> 25% (w/w)			
$R = \frac{V_W}{V_O}$	0.16–0.97	–	1.13–2.93
$W = \frac{m_W}{m_{SF}}$	0.56–3.38		3.95–7.74
10–25% (w/w)			
$R = \frac{V_W}{V_O}$	0.04–0.11	1.00–1.33	1.60–1.73
$W = \frac{m_W}{m_{SF}}$	0.10–0.30	1.53–2.03	2.44–2.64

that influences their physical or chemical properties. Their novel or unusual physical properties are mainly due to the finite-size effect: electronic bands are gradually converted to molecular orbital as the size decreases.

The difference in the peak position of the electronic spectra is related with the size effect of dispersed droplets in the bulk phase. When a three-dimensional square-well potential with the length of L in x, y, and z directions is of the quantum size, the energy of an electron, E, confined within the potential, will be given by the following equation [45,46]:

$$\Delta E = (3\hbar\pi^2)/\left(2mL^2\right) \quad (1)$$

where m is the static mass of an electron ($9.10938 \cdot 10^{-31}$ kg).

The size of the aggregates in the micelles, L, may be obtained from ΔE (equation (1)), and is the difference between the position of BTB peak in various solvents and that in colloidal systems (micelles or microemulsions) (Tables 4–7).

Size evaluation of colloidal aggregates is based on the shifts of absorption maxima of BTB VIS spectra, and this was possible since the microemulsions have a very small degree of polydispersity.

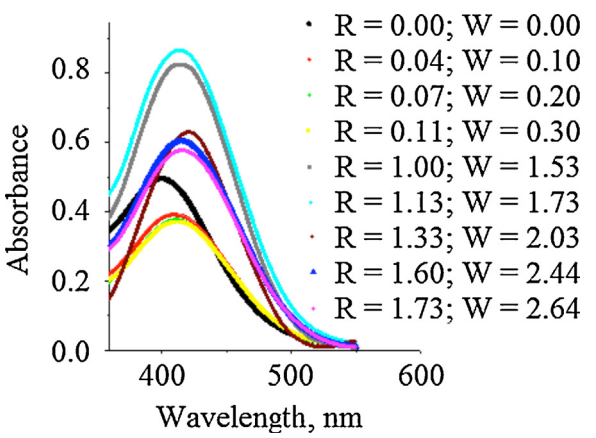

Fig. 5. (Color online.) Absorption spectra of BTB in the water/Brij 30/TEOS system before and after phase separation.

Based on the spectral investigations of the systems with TEOS, apparently BTB remains attached to the surfactant OE groups (no BTB solubilisation in water or oil drops was observed). As the probe is localized in the inner surfactant OE groups, the absorption maximum of BTB in TEG (λ_{max} = 416.4 nm) has been chosen as the reference.

Finally, a decrease in the aggregates sizes can be observed by raising the amount of added water to the system for water-in-oil microemulsions. The same evolution can also be noticed for oil-in-water microemulsions, meaning a decrease in size with raising the water ratio. The existence of microemulsions is thus confirmed by the aggregate sizes and therefore the definition of microemulsion as an isotropic system containing colloidal assemblies with dimensions smaller than 100 nm, spread in a continuous environment can be applied to this kind of systems as well.

This comprehensive approach and all the obtained results allow one to pattern microemulsion-based silica templates, by controlling the droplet type and size and directing the silica network formation around them.

Table 4
Size of aggregates in WIV (water-in-oil) microemulsion.

	W IV (water-in-oil)			
$R = V_W/V_{TEOS}$	0.21	0.31	0.41	0.52
$W = m_W/m_{SF}$	0.15	0.30	0.61	0.76
C_{SF}, % (w/w)	38.19	36.10	32.54	31.01
λ, nm	409.80	410.40	411.20	411.60
10^{21} ΔE, J	7.57	6.92	5.89	5.51
L, nm	4.90	5.10	5.50	5.70

Table 5
Size of aggregates in WIV (oil-in-water) microemulsion.

	W IV (oil-in-water)			
$R = V_W/V_{TEOS}$	1.98	2.56	3.14	3.53
$W = m_W/m_{SF}$	1.65	2.13	2.61	2.94
C_{SF}, % (w/w)	28.73	25.23	22.49	20.97
λ, nm	413.80	412.80	412.20	410.80
10^{21} ΔE, J	2.74	4.03	4.82	6.39
L, nm	8.10	6.70	6.10	5.30

Table 6
Size of aggregates in WI (oil excess, oil-in-water) microemulsion.

	W I (oil excess, oil-in-water)			
$R = V_W/V_{TEOS}$	0.77	0.84	0.88	1.03
$W = m_W/m_{SF}$	3.92	4.27	5.56	6.49
C_{SF}, % (w/w)	10.00	9.66	7.78	7.26
λ, nm	412.20	410.60	408.80	397.40
10^{21} ΔE, J	4.72	6.58	8.75	22.69
L, nm	6.02	5.20	4.50	2.80

Table 7
Size of aggregates in WII (water-in-oil, water excess) microemulsion.

	W II (water-in-oil, water excess)			
$R = V_W/V_{TEOS}$	0.90	1.08	1.17	1.26
$W = m_W/m_{SF}$	1.88	2.26	2.44	2.63
C_{SF}, % (w/w)	20.14	18.73	18.09	17.49
λ, nm	412.8	413.80	414.00	414.20
10^{21} ΔE, J	4.10	2.79	2.71	2.54
L, nm	6.60	8.00	8.20	8.40

4. Conclusion

A comprehensive pool of information and tools required for the design and synthesis of inorganic and hybrid silica-based nanomaterials, nanoparticles or films, using silica-microemulsion templates, are provided by the present work, such as microemulsion formulation compositions, temperature, type, *polarity*, and size of nanodroplets.

All studied systems, based on a non-ionic surfactant (Brij 30) and different silica precursors (MTEOS, TEOS, PTEOS), do form high-solubilizing performance microemulsions that are able to solubilize approximately equal amounts of alcoxides and water, with less than 10–20% (w/w) Brij 30 as the surfactant. By corroborating the information obtained from phase diagrams at room temperature with that of size effects revealed by VIS absorption molecular probes (bromthymol blue dye), the PIP, meaning the phase transition point from water-in-oil to oil-in-water microemulsion, was clearly established. The temperature-dependent phase behaviour in water-Brij 30-alcoxide systems has been shown by Khalweit diagrams and consequently the PIT was estimated as being close to 315 K, for both alchil (TEOS) and aril (PTEOS) types of alcoxides. By drawing phase diagrams at a temperature higher than PIT, the formation of a bicontinuous microemulsion as WIII type is proved.

Finally, the presented results highlight the interest to use microemulsion silica-based templates to obtain a wide range of mesoporous silica-based inorganic and hybrid nanomaterials. With all of these in mind, the large-scale application of the silica-microemulsion template-based technique for silica-based composites materials fabrication becomes more realistic.

Acknowledgements

The work has been funded by the Sectoral Operational Programme Human Resources Development 2007-2013 of the Romanian Ministry of Labour, Family and Social Protection through the Financial Agreement POSDRU/107/1.5/S/76909.

The authors would also like to thank for the financial support from ANCS, PN II contract No. C2-07/01.03.2012, project acronym NANOLIGHT.

Appendix A. Supplementary data

Supplementary data associated with this article can be found, in the online version, at http://dx.doi.org/10.1016/j.crci.2013.09.018.

References

[1] K. Kouachi, G. Lafaye, C. Especel, O. Cherifi, P. Marécot, J. Mol. Catal. A: Chem. 308 (2009) 142–149.
[2] K. Kouachi, G. Lafaye, C. Especel, O. Cherifi, P. Marécot, J. Mol. Catal. A: Chem. 280 (2008) 52–60.
[3] K. Sowri Babu, A. Ramachandra Reddy, C. Sujatha, K. Venugopal Reddy, Ceram. Int. 38 (2012) 5949–5956.
[4] Y. Jin, A. Li, S.G. Hazelton, S. Liang, C.L. John, P.D. Selid, D.T. Pierce, J.X. Zhao, Chem. Rev. 253 (2009) 2998–3014.
[5] I. Fechete, Y. Wang, J.-C. Védrine, Catal. Today, 189 (2012) 2–27.
[6] G. Corro, U. Pal, N. Tellez, Appl. Catal., B 129 (2013) 39–47.
[7] K. Nam, S. Lim, S.K. Kim, S.H. Yoon, D.H. Jung, Int. J. Hydrogen Energy 37 (2012) 4619–4626.
[8] G.A. Santos, C.M.B. Santos, S.W. da Silva, E.A. Urquieta-González, P.P.C. Sartoratto, Colloids Surf., A 395 (2012) 217–224.
[9] G.A.H. Mekhemer, H.M.M. Abd-Allah, S.A.A. Mansour, Colloids Surf., A 160 (1999) 251–259.
[10] S. Eriksson, U. Nylén, S. Rojas, M. Boutonnet, Appl. Catal., A 265 (2004) 207–219.
[11] M. Hussain, N. Abbas, D. Fino, N. Russo, Chem. Eng. J. 188 (2012) 222–232.
[12] S.X. Zhang, T.Y. Ma, T.Z. Ren, Z.Y. Yuan, Chem. Eng. J. 171 (2011) 368–372.
[13] X. Chen, K.F. Lam, K.L. Yeung, Chem. Eng. J. 172 (2011) 728–734.
[14] F. Zhengping, Y. Beifang, L. Lin, D. Weiwei, J. Chong, W. Wan, J. Phys.: Condens. Matter 15 (2003) 2867–2873.
[15] R.J. Martínez-Palma, R. Guerrero-Lemus, J.D. Moreno, J.M. Martínez-Duart, Solid-State Electron. 43 (1999) 1153–1157.
[16] F. Pena-Pereira, R.M.B.O. Duarte, A.C. Duarte, Trends Anal. Chem. 40 (2012) 90–105.
[17] T. Tsoncheva, J. Rosenholm, M. Linden, F. Kleitz, M. Tiemann, L. Ivanova, M. Dimitrov, D. Paneva, I. Mitov, C. Minchev, Microporous Mesoporous Mater. 112 (2008) 327–337.
[18] L. Lizama, J.C. Amezcua, T. Klimova, Stud. Surf. Sci. Catal. 174 (2008) 1351–1354.
[19] F. Boubekr, A. Davidson, S. Casale, P. Massiani, Microporous Mesoporous Mater. 141 (2011) 157–166.
[20] S. Jun, R. Ryoo, J. Catal. 195 (2000) 237–243.
[21] X. Hu, M.L. Foo, G.K. Chuah, S. Jaenicke, J. Catal. 195 (2000) 412–415.
[22] S.K. Park, V. Kurshev, Z. Luan, C. Wee Lee, L. Kevan, Microporous Mesoporous Mater. 38 (2000) 255–266.
[23] W.S. Ahn, D.H. Lee, T.J. Kim, J.H. Kim, G. Seo, R. Ryoo, Appl. Catal., A 181 (1999) 39–49.
[24] R. Burch, N. Cruise, D. Gleeson, S.G. Tsang, Chem. Commun. (1996) 951–952.
[25] W. Zhao, L. Kong, Y. Luo, Q. Li, Microporous Mesoporous Mater. 100 (2007) 111–117.
[26] F. Gao, Y.H. Zhang, C.L. Wang, C. Wu, Y. Kong, B. Zhao, L. Dong, Y. Chen, J. Nanosci. Nanotechnol. 7 (2007) 4508–4514.
[27] M. Pirouzmand, M.M. Amini, N. Safari, J. Colloid Interface Sci. 319 (2008) 199–205.
[28] I. Fechete, B. Donnio, O. Ersen, T. Dintzer, A. Djeddi, F. Garin, Appl. Surf. Sci. 257 (2011) 2791–2800.
[29] K. Anas, K.K. Mohammed Yusuff, Appl. Catal., A 264 (2004) 213–217.
[30] O. Collart, P. Van Der Voort, E.F. Vansant, E. Gustin, A. Bouwen, D. Schoemaker, R. Ramachandra Rao, B.M. Weckhuysen, R.A. Schoonheydt, Phys. Chem. Chem. Phys. 1 (1999) 4099–4104.
[31] M. Yonemitsu, Y. Tanaka, M. Iwamoto, Chem. Mater. 9 (1997) 2679–2681.
[32] M. Yonemitsu, Y. Tanaka, M. Iwamoto, J. Catal. 178 (1998) 207–213.

[33] M. Mihaly, A. Comanescu, A. Rogozea, C. Pirvu, I. Rau, J. Soc. Photo-Optical Instr. Eng. (2009), doi:10.1117/12.828853.
[34] M. Mihaly, A.F. Comanescu, A.E. Rogozea, E. Vasile, A. Meghea, Mater. Res. Bull. 46 (2011) 1746–1753.
[35] M. Mihaly, A. Rogozea, A. Comanescu, E. Vasile, A. Meghea, J. Optoelectron. Adv. Mat. 12 (2010) 2097–2105.
[36] D.P. Macwan, P. Dave, S. Chaturvedi, J. Mater. Sci. 46 (2011) 3669–3686.
[37] A. Karami, J. Iran. Chem. Soc. 7 (2010) S154–S160.
[38] C.L. Chang, H.S. Fogler, Langmuir 13 (1997) 3295–3307.
[39] T. Aubert, F. Grasset, S. Mornet, E. Duguet, O. Cador, S. Cordier, Y. Molard, V. Demange, M. Mortier, H. Haneda, J. Colloid Interface Sci. 341 (2010) 201–208.
[40] C. Destrée, J.B. Nagy, Adv. Colloid Interface Sci. 123–126 (2006) 353–367.
[41] N.L. Olteanu, A. Meghea, UPB Sci. Bull., Series B 75 (4) (2013) 79–90.
[42] C.L. Sassen, A.G. Casielles, T.W. Deloos, J.D. Arons, Fluid Phase Equilib. 72 (1992) 173–188.
[43] C. Stubenrauch, Microemulsion, Ed. Wiley-VCH, Weinheim, Germany, 2009.
[44] B. Sahraoui, M. Pranaitis, K. Iliopoulos, M. Mihaly, A.F. Comanescu, M. Moldoveanu, I. Rau, K. Kazukauskas, Appl. Phys. Lett. 99 (2011) 243304 [3 p].
[45] P. Atkins, J. De Paula, Physical chemistry, Oxford University Press, 2006
[46] M. Mihaly, I. Lacatusu, A. Meghea, Rev. Chim. 58 (2007) 929–933.